Chapter 2
Review of Single-Crystal Silicon Properties

Abstract A review of silicon single crystal properties is essential to understanding silicon components. The objective of this chapter is to highlight only those semiconductor properties that are most important to analog and digital silicon device operation and characteristics discussed in the following chapters. The chapter covers carrier concentrations and thermal-equilibrium statistics, carrier transport under low-and high-field conditions, and minority-carrier lifetime and diffusion length.

2.1 Introduction

Solids and liquids contain 10^{22}–10^{23} atoms/cm^3. In crystalline solids, the elements are stacked in a periodic pattern. When the periodicity extends throughout the sample, one speaks of a *single crystal* (or mono-crystal), as opposed to a poly crystal which consists of small crystallites, called *grains,* arranged in random directions and adhering together at *grain boundaries*. Non-crystalline solids are said to be *amorphous*. Typically, solids assume the crystalline state because this is the packing of minimum energy.

A review of silicon single-crystal properties is essential to understanding silicon components. The objective of this chapter is to highlight only those semiconductor properties that are most important to analog silicon device operation and characteristics discussed in the following sections. Detailed treatments of semiconductor physics can be found in Refs. [1–6] at the end of the chapter. Important properties of the silicon crystal are given in the Appendix B.

2.2 Crystal Structure

Silicon, germanium, and carbon crystals belong to the cubic crystal system and have the diamond structure represented in three dimensions in Fig. 2.1 and in a two-dimensional projection in Fig. 2.2. The crystal consists of stacked cubes like that

B. El-Kareh and L.N. Hutter, *Silicon Analog Components*,
DOI 10.1007/978-1-4939-2751-7_2

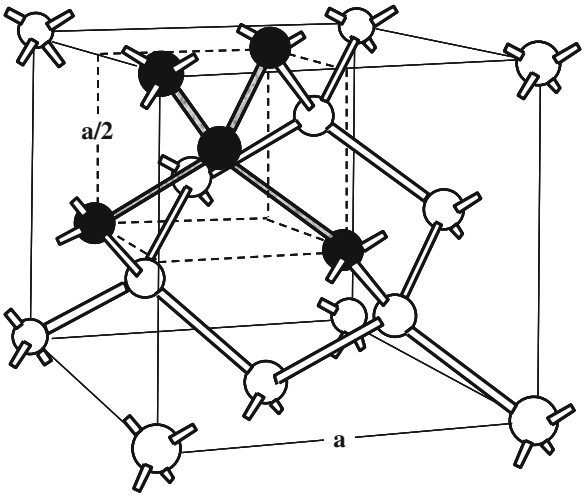

Fig. 2.1 Three-dimensional representation of unit diamond cell. *Dark atoms* define the unit sub-cell. Lattice constant $a = 0.543$ nm

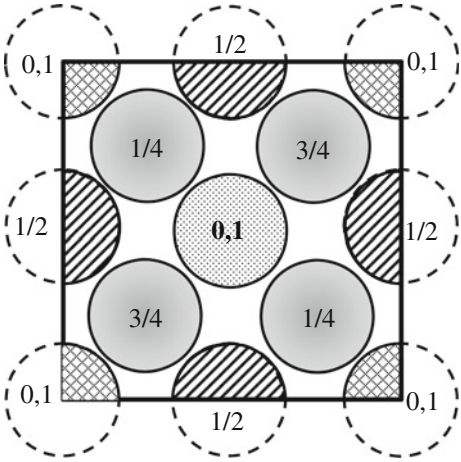

Fig. 2.2 Projection of atoms in Fig. 1.1 onto the plane of the page. *Numbers* indicate vertical distances in fractions of lattice constant a from the page, which is taken to be zero

shown in Fig. 2.1. Each atom is surrounded by four others with which it forms *covalent bonds*, i.e., bonds between two adjacent atoms are formed by two valence electrons, one from each atom contributing to the bond. The bonds are visualized as localized bars along which electrons shuttle back and forth with opposite spins, as illustrated schematically in Fig. 2.3a. This type of bonding is very strong, highly localized, and directional because the distribution of valence electrons becomes shifted to the nearest neighbors. The unit cell configuration in a diamond crystal is best described by projecting the cube onto a two-dimensional plane, as shown in Fig. 2.2 [1]. The plane of the paper is chosen as one of the cube planes. The numbers define the location of the atom centers relative to the plane of the paper in fraction of the cube edge a. For example, atoms located at the centers of cube faces

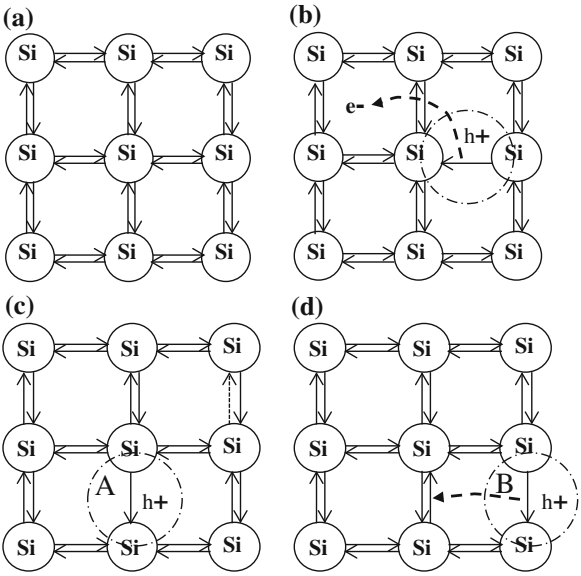

Fig. 2.3 Schematic representation of Si bonds. **a** Crystal at about 0 K, all bonds in place. **b** Thermal generation of electron–hole pair. **c**, **d** Illustration of thermal motion of a hole

normal to the page are labeled ½. In a unit cube, there are 8 corner atoms, each shared between 8 adjacent cubes; 6 face-centered atoms, each shared between two adjacent cubes; and 4 full atoms within the cube. One should remember that the structure is three dimensional and that the bonds form a continuous three-dimensional chain throughout the crystal. The electrons are not constrained to one particular bond. Instead, they can move throughout the crystal, exchanging places with other valence electrons without creating current. Thus, the bonding electrons belong to the entire crystal rather than to local atoms.

At normal operating temperatures, atoms occupy, on the average, fixed positions relative to each other. The atoms are, however, in constant vibrations about their equilibrium positions.

2.3 Energy-Gap and Intrinsic Carrier Concentration

When a pure silicon crystal is at near 0 K, all valence electrons remain locally bound to their covalent bonds since they do not have sufficient energy to break loose (Fig. 2.3a). In this case, no free electrons are present and the crystal behaves like a perfect insulator.

As the temperature is increased, the amplitude of vibration of lattice atoms also increases around their equilibrium positions. A fraction of the vibrational energy is transferred to valence electrons. Some electrons can acquire sufficient energy to break loose from their bonds and move randomly in the crystal (Fig. 2.3b). A vacancy is left where an electron breaks loose from a bond. The vacancy behaves

like a positive carrier that is conveniently called a *hole* that randomly moves in the crystal, independently of the free electron. The motion of holes is illustrated in Fig. 2.3c, d. Figure 2.3c shows a hole at a random position *A*. A nearby *bound* electron can move into the hole, completing the bond in Fig. 2.3c, eliminating that hole and creating a new one nearby, as shown in Fig. 2.3d, and so on. It is convenient to describe this process as the motion of a hole although it is a *bound electron* that moves in the opposite direction. The charge of electrons and holes are equal in magnitude but opposite in sign. Free electrons and holes are generated *in pairs* and their number increases with increasing temperature. Under normal operating conditions, the silicon atoms remain fixed around their equilibrium positions. The energy required to break a silicon bond is about 1.1 eV at 25 °C.[1] The crystal as a whole remains neutral. During their random motion, free electrons and holes may recombine, thus annihilating a positive and a negative charge at the same time. In pure silicon, the concentrations of electrons and holes remain equal since their *generation* and *recombination* occurs in pairs. In such a case, silicon is said to be *intrinsic*.

2.3.1 Energy Band Model

Energy bands in semiconductors are discussed extensively in reference books on solid-state physics [1–6]. The sole objective of this section is to highlight, in simple terms, the energy-band model concepts that are most pertinent to understanding the properties of silicon devices.

An electron in vacuum is allowed to occupy a continuum of energy levels, similar to the classical case of molecules in an atmospheric column that can occupy any energy level without restrictions. From quantum mechanics, it is known that when an electron is *bound*, e.g., as in an isolated hydrogen atom, it is allowed only discrete energy levels separated by energy gaps. When two hydrogen atoms are far from each other, they behave as two isolated entities with independent, identical sets of discrete energy levels. As the *atoms* are brought close to each other, their wave functions begin to overlap so that the electrons of the two atoms begin to interact. Electrons in the first atom can also occupy energy levels in the second and vice versa. A study of energy levels shows that, in the limit, when a hydrogen molecule is formed, each energy level of the isolated hydrogen atom splits into *two* levels, one above and one below the energy level in an isolated atom.

In a silicon crystal of N identical lattice atoms, there exists the possibility of exchange of every valence electron with valence electrons of the remaining $N - 1$ atoms. One *expects* then that each energy level of the isolated atom would split in the

[1]One electron volt (eV) is the energy dissipated or acquired by one electron that goes through a potential difference of 1 V. Since the charge of one electron is 1.6×10^{-19} Coulomb, 1 eV = 1.6×10^{-19} J. In this book, eV and cm are frequently used in place of J and m, as a convenient departure from SI units.

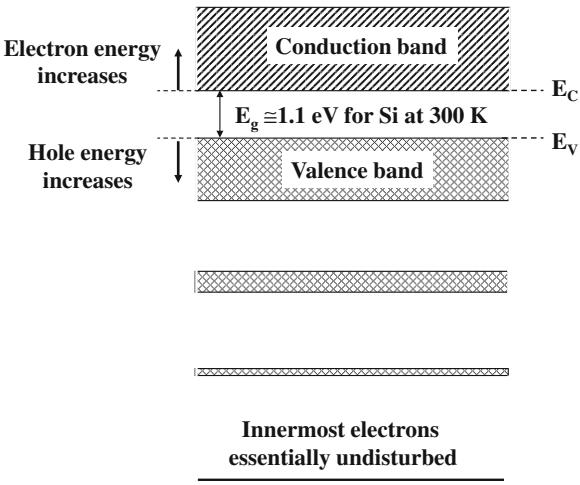

Fig. 2.4 Simplified energy-band diagram illustrating the increase in band width with increasing electron energy

crystal into N energy levels, each of which can be occupied by two electrons of opposite spins. Since N is a very large number ($\sim 10^{23}$ cm^{-3}), the levels are too close to each other to be distinguished. They are thus described by a band of energy levels, bounded by a maximum and minimum level (Fig. 2.4). The energy levels of innermost electrons remain sharp because the probability for them to interact is very small. The width of a band increases as the electron energy increases. Of primary interest for conduction are the uppermost two bands, the *conduction band* of free electrons,[2] and the band just below the conduction band, referred to as the *valence band*, i.e., the band of bound electrons. In terms of the band diagram in Fig. 2.4, the energy to break a bond is the *energy gap* (or forbidden gap) E_g. The energy gap is a function of the lattice constant [2]. One would thus expect E_g to depend somewhat on temperature and pressure. The temperature dependence of E_g is approximated as [7]

$$E_g \cong 1.187 - 3.6 \times 10^{-4} T \ \text{eV} \tag{2.1}$$

In semiconductors near absolute zero, the valence band is full (all bound electrons in place) and the conduction band is empty, so the crystal behaves like a perfect insulator. As the temperature increases, some electrons acquire sufficient energy from crystal vibrations to overcome the energy gap E_g and are elevated from the valence band to the conduction band where they are free to move. Holes are created in the valance band where electrons are missing. Since most transitions occur between the band edges, only the bottom of the conduction band, E_C, and the top of the valence band, E_V, will be considered (Fig. 2.5). The silicon band structure

[2]Although the electron is free to move, it is still bound to the crystal. Electrons in the conduction band are sometimes described as quasi-free, i.e., behaving as if they were free. For simplicity, the term "free electron" will be used in this book to describe an electron in the conduction band.

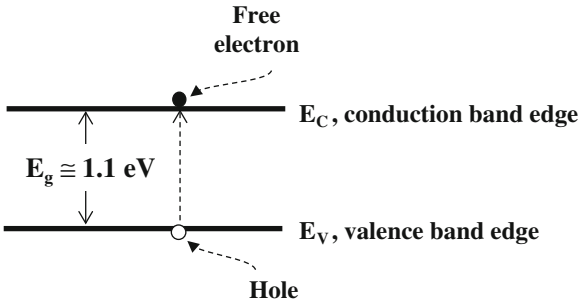

Fig. 2.5 Simplified band diagram. At near 0 K, the valence band is full, the conduction band is empty. As temperature increases, the number of electron transitions from E_V to E_C increases

is rather complex. Unless otherwise stated, the simplified model in Fig. 2.5 will be used for most discussions.

For a fixed and uniform temperature throughout the crystal and without external disturbances, such as applied voltage directly to the crystal, light or radiation, the crystal is said to be at *thermal equilibrium*. For each temperature, there is an associated equilibrium concentration of electrons, $\overline{n}$ and holes, $\overline{p}$. For intrinsic silicon

$$\overline{n} = \overline{p} = n_i \ \text{cm}^{-3} \tag{2.2}$$

$$\overline{pn} = n_i^2 \ \text{cm}^{-6} \tag{2.3}$$

where the bars indicate equilibrium values and n_i is the *intrinsic carrier concentration*, an important property of a semiconductor.

2.3.2 The Boltzmann Distribution

From the kinetic theory of gases, it is known that the average energy of a particle is $3kT/2$, where k is the *Boltzmann's constant* ($k = 8.625 \times 10^{-5}$ eV/K $= 1.380 \times 10^{-23}$ J/K), and T is the absolute temperature in K. It is also known that the probability P_i of an atom or molecule being at an energy level E_i relative to the probability P_o of being at an energy level E_o is

$$\frac{P_i}{P_o} = \frac{e^{-E_i/kT}}{e^{-E_o/kT}} = e^{-(E_i - E_o)/kT} \tag{2.4}$$

The inverse exponential dependence indicates that, for a given temperature, the probability decreases as the energy difference increases. This means that it is more likely to find atoms or molecules at low energy than at high energy. The expression also indicates the probability increases as the temperature is increased.

One classical example is the distribution of molecules acting under the influence of gravity in a column of an idealized atmosphere which is assumed to be at a constant temperature. The number of molecules at a height Δh above a reference height h is

$$N_{h+\Delta h} = N_h e^{-mg\Delta h/kT} = N_h e^{-\Delta E/kT} \tag{2.5}$$

In the above relation, $N_{h+\Delta h}$ is the number of molecules at a height Δh above h, N_h is the number of molecule at a height h, m is the molecular mass, g is the acceleration due to gravity, and $mg\Delta h$ is the increase ΔE in potential energy as the molecule rises from h to $h + \Delta h$. The exponential on the right of (2.5) is called the *Boltzmann factor*.

2.3.3 Fermi–Dirac Distribution and Density of States

The Boltzmann distribution function is applicable to atoms and molecules because they can occupy any energy level without restrictions on how many occupy the *same* energy level. Electrons in a crystal are, however, subject to Pauli's exclusion principle and hence allowed to occupy only discrete energy levels, called *states*, separated by forbidden gaps. Thus, statistics applied for the distribution of electrons and holes is different than used for the distribution of atoms or molecules. At thermal equilibrium, the probability that an energy level E be occupied by an electron is given by the so-called *Fermi–Dirac distribution function* [1–6]

$$f(E) = \frac{1}{1 + e^{(E-E_F)kT}} \tag{2.6}$$

where $f(E)$ is the probability of occupancy (from 0 to 1) and E_F is the *Fermi level*, a *hypothetical* reference energy level that depends on temperature, and also on dopant concentration as discussed in the next section. The Fermi level does not imply an allowed energy level. It is determined by the requirement that the probability of occupancy for all energy levels above and below E_F satisfies (2.6), and that the crystal as a whole remains neutral. Since an energy level can be either occupied or not occupied by an electron, the probability that a level E is *not* occupied by an electron is given by

$$1 - f(E) = \frac{1}{1 + e^{(E_F-E)kT}} \tag{2.7}$$

At an energy $E = E_F$, the exponential in the denominator goes to 1 and the probability $f(E) = 0.5$ (or 50 %). This means that there is an equal probability that the level E will be occupied or vacant.

In a semiconductor, the Fermi level is typically located within the forbidden gap. As E_F approaches E_C, $(E_C - E_F)$ decreases and the probability of finding an

electron at E_C increases while the probability of *not* finding an electron at E_V, i.e., finding a hole at E_V, decreases. This is because the magnitude of the exponential in the denominator of (2.6) decreases and the exponential in (2.7) increases. Similarly, as E_F approaches E_V, $(E_F - E_V)$ decreases and $E_C - E_F$ increases. In this case, the probability of non-occupancy at E_V increases, i.e., the probability of finding a hole at E_V increases, while the probability of finding an electron at E_C decreases.

For intrinsic silicon, E_F is close to half-way between E_C and E_V, indicating that there is nearly equal probability of finding an electron at E_C and a hole at E_V. This particular level is referred to as the *intrinsic energy level*, E_i. For energies larger than about $3kT$ above E_F, (2.6) can be approximated as

$$f(E) = e^{-(E-E_F)/kT} \tag{2.8}$$

because the "1" in the denominator becomes negligible compared to the exponential. Similarly, for $(E_F - E)$ larger than about $3kT$, (2.7) simplifies to

$$f(E) = e^{-(E_F-E)/kT} \tag{2.9}$$

Because of their similarity to (2.5), the distributions (2.8) and (2.9) are referred to as *Boltzmann approximations*. Since in intrinsic silicon $E_C - E_F \cong E_F - E_V \cong 0.55$ eV $\cong 21kT$, the Boltzmann approximation is applicable.

At a given temperature, the number of electrons in a small energy interval of a band depends on two factors: The probability that an electron will have this energy, and on the number of available *energy states* in that interval. Each band in Fig. 2.4 consists of a large number of states distributed within the band, but since in the most cases transitions occur predominantly between band edges, *effective density of states* N_C and N_V, at band edges E_C and E_V are conveniently introduced to estimate the concentrations of conduction electrons and holes.

In the temperature range of 200–425 K, the effective density of states for electrons and holes can be approximated as [7]

$$N_C \cong 2.80 \times 10^{19} \left(\frac{T}{300}\right)^{1.5} \text{ cm}^{-3} \tag{2.10}$$

$$N_V \cong 1.02 \times 10^{19} \left(\frac{T}{300}\right)^{1.5} \text{ cm}^{-3} \tag{2.11}$$

Since by definition there should be no states within the forbidden gap, no electrons should be found within the gap even though the probability of occupancy is finite. Real crystals, however, do not follow this rule because of unavoidable "foreign materials" and defects, as will be discussed in Sect. 2.6 and in the following sections.

When the Boltzmann approximation applies, the electron concentration is found as the product of (2.8) and (2.10):

$$\overline{n} = N_C e^{-(E_C - E_F)/kT} \cong 2.80 \times 10^{19} \left(\frac{T}{300}\right)^{1.5} e^{-(E_C - E_F)/kT} \ \text{cm}^{-3} \tag{2.12}$$

Similarly, the concentration of holes is found from (2.9) and (2.11) as:

$$\overline{p} = N_V e^{-(E_F - E_V)/kT} \cong 1.02 \times 10^{19} \left(\frac{T}{300}\right)^{1.5} e^{-(E_F - E_V)/kT} \ \text{cm}^{-3} \tag{2.13}$$

The $\overline{pn}$ product is found from (2.12) and 2.13) as

$$\overline{pn} = n_i^2 = N_V N_C e^{-(E_C - E_V)/kT} = N_V N_C e^{-E_g/kT} \ \text{cm}^{-6} \tag{2.14}$$

Example 2.1 How close to the mid-gap is E_F located in intrinsic silicon at thermal equilibrium? Assume 300 K.

Solution
Since silicon is intrinsic, $\overline{n} = \overline{p}$ and E_F can be found by equating (2.12) and (2.13) as

$$E_F = E_i = \frac{E_C + E_V}{2} + \frac{kT}{2} \ln \frac{N_V}{N_C} \approx \frac{E_g}{2} + \frac{0.02586}{2} \ln \frac{1.04}{2.8} \approx 0.55 - 0.013 \ \text{eV}$$

E_F is about 13 meV below mid-gap; not exactly at mid-gap because of the difference between N_C and N_V.

Example 2.2 Use the values at 300 K in Table 2.1 to calculate n_i for silicon (Si), germanium (Ge), and gallium–arsenide (GaAs).

Solution
Substituting the values in Table 2.1 in (2.14) gives:

	Si	Ge	GaAs
n_i (cm^{-3})	1.4×10^{10}	2.3×10^{13}	1.8×10^{6}

Taking the variation of E_g with temperature in (2.1) into account, the temperature dependence of n_i in silicon can be approximated as

$$n_i = 2.63 \times 10^{16} T^{1.5} e^{-6885/T} \ \text{cm}^{-3} \tag{2.15}$$

A plot of n_i versus temperature is shown in Fig. 2.6.

Table 2.1 Values for E_g, N_C, and N_V for Si, Ge, and GaAs at 300 K

	Si	Ge	GaAs
E_g (eV)	1.08	0.66	1.42
N_C (cm^{-3})	2.80×10^{19}	1.04×10^{19}	4.70×10^{17}
N_V (cm^{-3})	1.02×10^{19}	6.00×10^{18}	7.00×10^{18}

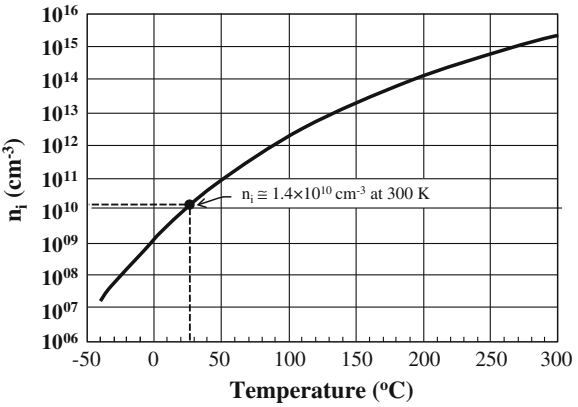

Fig. 2.6 Temperature dependence of n_i

2.4 Doping

By adding small and controlled amounts of certain elements to the otherwise pure silicon, the crystal can be *doped* to have more free electrons than holes and vice versa. To be active, the dopants must occupy substitutional sites, i.e., occupy a lattice site normally occupied by silicon. Doping is performed by implantation and diffusion and discussed in more detail in [8]. Of particular importance to silicon devices is doping with elements from the third and fifth columns of the periodic table (Fig. 2.7).

2.4.1 Dopants from the Fifth Column—Donors

Phosphorus, arsenic, antimony, and bismuth are elements of the fifth column (Group V). These elements have five electrons in their outer shell, i.e., five valence electrons. When they occupy a substitutional site in silicon, only four of the valence electrons are needed to complete the covalent bonding in the crystal. The fifth electron does not contribute to the bonding (Fig. 2.8a). The energy required to set the fifth electron free is very small so that, under normal operating temperatures and for concentrations less than about 10^{18} cm^{-3}, nearly all dopants release (or donate) their fifth electron to the crystal. After donating an electron, the donor cannot lose another one. Each *donor* left behind becomes a fixed positive ion with four bound valence electrons, the same as the original silicon atom. Note that by ionizing the donor, a conduction electron is generated *without creating a hole*. Thus, if one assumes that all donor atoms are ionized, $N_D^+ \cong N_D$.The crystal becomes rich in electrons, N-type, but remains neutral as a whole. Neutrality requires that

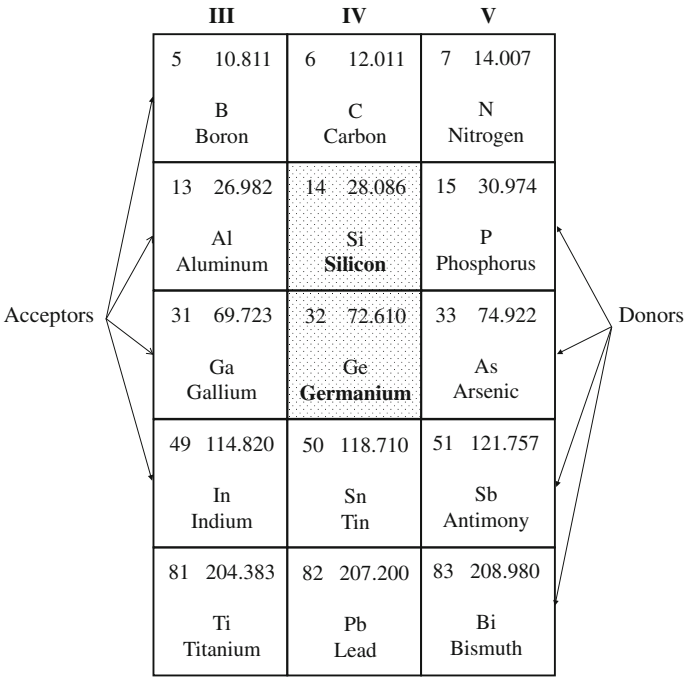

Fig. 2.7 Important semiconductor elements

$$\overline{n} = \overline{p} + N_{\mathrm{D}}^{+} \ \mathrm{cm}^{-3} \tag{2.16}$$

At temperatures below approximately 100 K, the probability for electrons to break loose from donors begins to decrease and an increasing fraction of electrons remains "frozen" to donors. High-dopant concentration effects are discussed in Chap. 5.

2.4.2 Dopants from the Third Column—Acceptors

Boron, aluminum, gallium, and indium are elements from the third column (Group III) in the periodic table. When substituted for silicon, the three available valence electrons in the outer shell take part in the bond structure, so that one electron is missing from the fourth bond. This vacant state is "attractive" to an adjacent bound electron that easily moves to fill it. Boron, aluminum, gallium, and indium "accept" the fourth electron, creating a hole where the filling electron came from *without producing a free electron* (Fig. 2.8b). After accepting one electron, an acceptor becomes a negatively ionized and cannot receive another one.

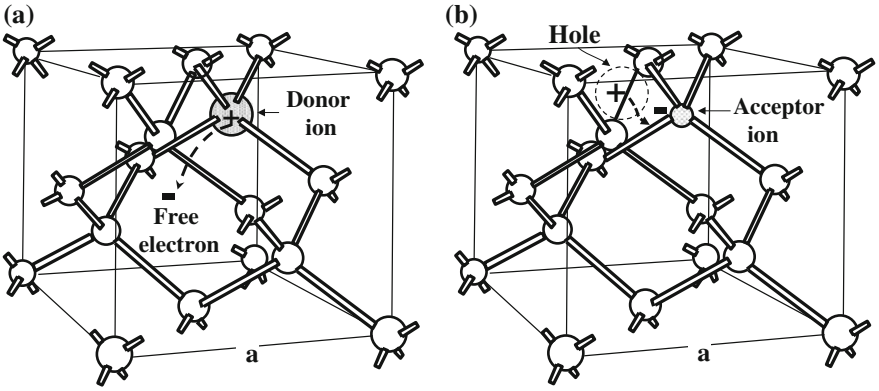

Fig. 2.8 Simplified model for dopants in silicon. **a** Free electron liberated from donor. **b** Nearby bound electron transferred to acceptor to complete bond, hole created

When silicon is doped with acceptors, the crystal becomes rich in holes or P-type. As with donors, the *ionization energy* of typical acceptors such as boron and indium is very small, so one can assume that, at normal operating temperatures and for concentrations below about 10^{18} cm^{-3}, all acceptor atoms are ionized, so $N_A^- \cong N_A$. Acceptors are fixed, negatively charged ions. Neutrality requires that

$$\overline{p} = \overline{n} + N_A^- \ \text{cm}^{-3} \tag{2.17}$$

The thermal equilibrium $\overline{pn}$ product in (2.3) is extremely useful in device analysis. While derived for intrinsic silicon, it also applies to doped silicon since it depends only on temperature and energy gap. The principle of mass action shows that when the concentration of one type of carriers increases, the concentration of other type must decrease so that the product remains constant. Thus, for N-type silicon, electrons are majority carriers, and holes minority carriers with

$$\overline{p} = \frac{n_i^2}{\overline{n}} \approx \frac{n_i^2}{N_D} \ \text{cm}^{-3} \tag{2.18}$$

Similarly, for P-type silicon, holes are majority carriers and electrons minority carriers of density

$$\overline{n} = \frac{n_i^2}{\overline{p}} \approx \frac{n_i^2}{N_A} \ \text{cm}^{-3} \tag{2.19}$$

Example 2.3 A silicon crystal is doped with 5×10^{17} phosphorus atoms/cm^3. Assume 25 °C and disregard point defects such as Si vacancies.

(a) Calculate the thermal equilibrium electron and hole concentrations.
(b) Estimate the number of broken bonds per cm^3.
(c) What is the distance between phosphorus atoms in units of silicon lattice constant?

Solution

(a) At 25 °C, it can be assumed that all phosphorus atoms are ionized and $\overline{n} \cong N_D = 5 \times 10^{17}\,cm^{-3}$. From Fig. 2.5, $n_i^2 \cong 2 \times 10^{20}\,cm^{-6}$. From (2.9), $\overline{p} = n_i^2/N_D \cong 2 \times 10^{20}/5 \times 10^{17} = 400\,cm^{-3}$.
(b) Since donors are ionized without breaking bonds, the number of broken bonds per cm^3 is the same as the concentration of holes.
(c) Since the P concentration is 5×10^{17}, each P atom occupies a volume of $1\ cm^3/5 \times 10^{17}$, i.e., it fits in a box having dimensions of $1/\sqrt{[3]}5 \times 10^{17}\,cm \cong 1.26 \times 10^{-6}cm$. In terms of lattice constant, this is $1.26 \times 10^{-6}/5.43 \times 10^{-8} \cong 23$ lattice constants.

2.4.3 Band Model for Impurities in Silicon

In terms of the band diagram, energy levels of donors such as arsenic (As), phosphorus (P), antimony (Sb), or bismuth (Bi) are represented by short bars just below the conduction band indicating discrete energy states E_D (Fig. 2.9). The numbers below the bars are the energies in meV (10^{-3} eV), measured from the donor level to the conduction band edge. The energy difference is so small that the probability for an electron to be raised from the donor level to the conduction band edge is very high.

When electrons previously bound to silicon atoms are captured by acceptor atoms to complete their fourth covalent bonds with silicon neighbors, they are only

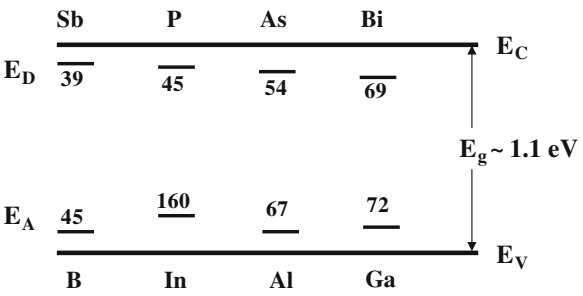

Fig. 2.9 Measured ionization energies in meV of donors and acceptors in silicon (adapted from [9]). Diagram is not to scale

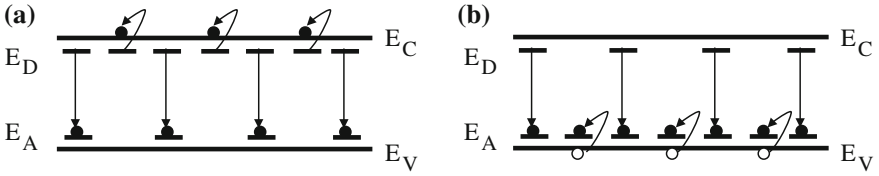

Fig. 2.10 Schematic representation of partially compensated impurities. **a** $N_D > N_A$, $n \approx N_D - N_A$. **b** $N_A > N_D$, $p = N_A - N_D$

a little less tightly held from being free than in silicon bonds. Acceptor levels are thus represented by short bars, indicating discrete energy states E_A just above the valence band (Fig. 2.9). The numbers above the bars are ionization energies (in meV) measured from the valence band edge. The probability for an acceptor energy level to be occupied by an electron coming from the valence band is almost 100 %. Thus, practically all acceptors are negatively ionized, each creating a hole in the valence band.

In most components, both donors and acceptors are present in the same region of the crystal. In this case, both donors and acceptors will be ionized, but only the *net*, i.e., the difference between their concentrations will be available for conduction (Fig. 2.10). The crystal is said to be *compensated*. In case donors and acceptors are exactly equal in concentration, all donors would be positively ionized without contributing free electrons, and all acceptors negatively ionized without contributing holes for conduction. In this case, $\overline{n} = \overline{p}$, i.e., the crystal is intrinsic but *not* pure. The neutrality condition for a compensated semiconductor is

$$\overline{p} + N_D^+ = \overline{n} + N_A^- \ \text{cm}^{-3} \tag{2.20}$$

For N-type silicon, E_F is above E_i and moves toward E_C as the net donor concentration is increased. This reflects an increase in electron concentration above the hole concentration (Fig. 2.11a). Similarly, for P-type silicon, E_F is below E_i and moves toward E_V as the net acceptor concentration is increased, indicating an increase in the hole concentration above the free electron concentration (Fig. 2.11b).

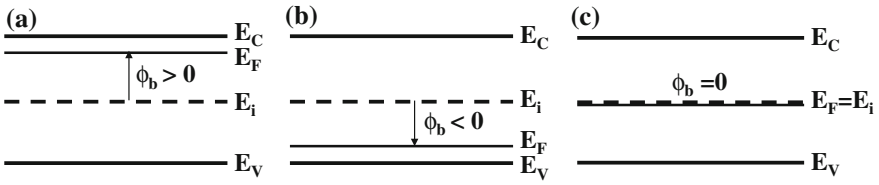

Fig. 2.11 Fermi level and definition of Fermi potential for **a** N-type, **b** P-type, and **c** intrinsic semiconductor

The difference ($E_F - E_i$) in Fig. 2.11 is divided by e (charge q) to convert the values from energy (eV) to V. $\phi_b = (E_F - E_i)/q$ is referred to as the "bulk" *Fermi potential*. For N-type silicon, E_F lies above the intrinsic level E_i and ϕ_b is positive. For P-type silicon, E_F lies below E_i and ϕ_b is negative. For intrinsic silicon $\phi_b = 0$ (Fig. 2.11c). The Fermi potential is an important parameter used in device analysis.

For intrinsic silicon $E_F = E_i$ and the Boltzmann approximation can be applied. The expression for the intrinsic carrier concentration simplifies to

$$n_i = N_C e^{-(E_C - E_i)/kT} \ \text{cm}^{-3} \tag{2.21}$$

or

$$n_i = N_V e^{-(E_i - E_V)/kT} \ \text{cm}^{-3} \tag{2.22}$$

For N-type silicon, the Fermi level above E_i can be determined by taking the ratio of (2.12) and (2.21) as

$$\frac{E_F - E_i}{q} = \phi_b = \frac{kT}{q} \ln \frac{\overline{n}}{n_i} \ \text{eV} \tag{2.23}$$

Similarly, for P-type silicon, Eqs. (2.13) and (2.22) give

$$\frac{E_i - E_F}{q} = -\phi_b = -\frac{kT}{q} \ln \frac{\overline{p}}{n_i} \ \text{eV} \tag{2.24}$$

For fully ionized dopants, the Fermi potential can also be expressed for N-type silicon as

$$\phi_b \cong \frac{kT}{q} \ln \frac{N_D}{n_i} \ \text{V} \tag{2.25a}$$

and for P-type silicon as

$$\phi_b \cong -\frac{kT}{q} \ln \frac{N_A}{n_i} \ \text{V} \tag{2.25b}$$

Example 2.4 A silicon crystal is doped with phosphorus at a uniform concentration of 2×10^{17} cm^{-3}. Assume full ionization of donors.

(a) Find the Fermi potential and carrier concentrations at −50, 27, and 150 °C.
(b) Repeat for a uniform boron concentration of 5×10^{16} cm^{-3}, and find the difference in Fermi potentials, $\phi_{bn} - \phi_{bp}$, between the phosphorus- and boron-doped regions.

Table 2.2 Fermi potentials for N-type and P-type silicon

N-type					
T (°C)	T (K)	n_i (cm^{-3})	ϕ_b (V)	$\overline{n}$ (cm^{-3})	$\overline{p}$ (cm^{-3})
-50	223	3.42×10^6	0.477	2×10^{17}	~ 0
25	300	1.47×10^{10}	0.425	2×10^{17}	1.09×10^3
150	423	1.95×10^{13}	0.337	2×10^{17}	1.91×10^9
P-type					
T (° C)	T (K)	ϕ_b (V)	$\overline{n}$ (cm^{-3})	$\overline{p}$ (cm^{-3})	$\phi_{bn} - \phi_{bp}$ (V)
-50	223	−0.450	~ 0	5×10^{16}	0.927
25	300	−0.389	4.35×10^3	5×10^{16}	0.814
150	423	−0.286	7.63×10^9	5×10^{16}	0.623

Solution

First, the intrinsic carrier concentration is found from (2.15). For a temperature of, e.g., −50 °C (223 K)

$$\begin{aligned} n_i &\approx 2.63 \times 10^{16} T^{1.5} e^{-6885/T} \\ &\approx 2.63 \times 10^{16} \times 223^{1.5} \times e^{-6885/223} \\ &\approx 3.42 \times 10^6 \quad cm^{-3} \end{aligned}$$

The Fermi potential for $N_D = 2 \times 10^{17}$ cm^{-3} is found from (2.25a) as

$$\phi_B \cong \frac{kT}{q} \ln \frac{N_D}{n_i} = 8.62 \times 10^{-5} \times 223 \times \ln \frac{2 \times 10^{17}}{3.42 \times 10^6} \cong 0.477 \quad V$$

The same procedure is repeated for the other temperatures and for boron-doped (P-type) silicon. Table 2.2 summarizes the results.

2.5 Carrier Transport

Electric current is defined as the flow of charge, i.e., the number of charged carriers transported per unit time across a given surface in a direction normal to it. The transport of carriers can occur in two ways:

(a) By *drift* , under the influence of an electric field. The field forces the otherwise randomly moving holes to drift in the direction of the field and electrons to drift opposite to the electric field.

(b) By *diffusion*, under the influence of a gradient in carrier concentration. In this case, carriers diffuse from regions of high concentration to regions of low concentration and tend to equalize concentrations within the region of diffusion.

Both drift and diffusion are involved in different degrees in the transport of carriers. In both cases, the electric current density depends on the concentration of charged carriers free to move and their velocities in the direction of current. For electrons,

$$j_n = qn\langle v\rangle \quad \text{A/cm}^2 \tag{2.26}$$

where j_n is the electron current density, n is the electron concentration, q is the electron charge ($q = 1.6 \times 10^{-19}$ C), and $\langle v\rangle$ is the average velocity in direction of current (cm/s).

Example 2.5 The electron density in a metal is approximately 10^{23} cm^{-3}. Assume a current density 0.5 mA/μm^2. At what velocity do the electrons travel through the metal? How does this compare with the velocity of electrons in silicon doped with $N_D = 10^{18}$ cm^{-3}, at the same current density?

Solution
The current density per cm^2 is $0.5 \times 10^{-3} \times 10^8 = 5 \times 10^4$ A/cm^2. The average velocity of electrons in the metal is found from (2.26) as

$$\langle v\rangle = \frac{5 \times 10^4}{1.6 \times 10^{-19} \times 10^{23}} = 3.13 \quad \text{cm/s}$$

For silicon doped with $N_D = 10^{18}$ cm^{-3}, the velocity is found as

$$\langle v\rangle = \frac{5 \times 10^4}{1.6 \times 10^{-19} \times 10^{18}} = 3.13 \times 10^5 \quad \text{cm/s}$$

2.5.1 Carrier Transport by Drift—Low Field

At a given temperature and in the absence of any disturbance, electrons and holes are in random motion in the crystal. The free carriers travel at high speed in all directions making random collisions with lattice atoms. They share their thermal motion with the crystal. The carriers, as a group, do not carry a net current in any direction because, on the average, as many move in one direction as in the other. This is illustrated in two dimensions in Fig. 2.12a. Each carrier acquires an average thermal energy of $3kT/2$ that is assumed to be lost after collisions for simplicity. At thermal equilibrium, the free-carrier average kinetic energy equals its average thermal energy $3kT/q$ so that the average thermal velocity, v_{th}, can be found from the relation

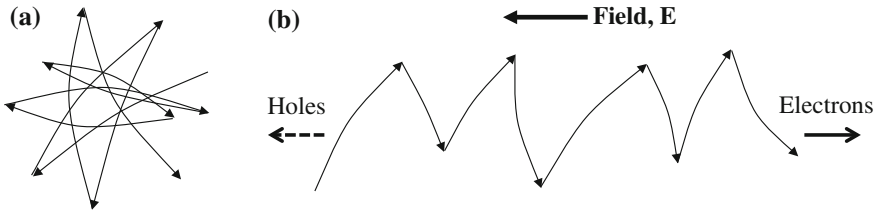

Fig. 2.12 **a** Schematic representation of random carrier motion at thermal velocity in absence of field; net current is zero. **b** Applied field E: organized electron drift in direction opposite to E

$$\frac{1}{2}m^* v_{\text{th}}^2 = \frac{3}{2}kT \text{ eV} \tag{2.27}$$

where m^* is the effective mass, which is almost the same as the free electron mass, and $\langle v_{\text{th}} \rangle$ is the average carrier thermal velocity ($v_{\text{th}} \cong 10^7$ cm/s at 300 K).

The lattice atoms vibrate about their mean positions but remain, on the average, in their lattice positions. The vibrations cause *collisions* with carriers, referred to as *scattering* events, randomly deflecting their motion.

When a voltage is directly applied to the crystal, a field is created causing a current and thus a departure from thermal equilibrium. The conventional direction of electric field is from positive to negative charge. Holes travel in the direction of electric field and electrons in a direction opposite to the field (Fig. 2.12b). For a small electric field, less than about 5×10^3 V/cm, the disturbance is very small so that the thermal equilibrium carrier distribution can still be assumed. Since electrons are negatively charged and move in opposite direction to holes, both currents have the same sign and the total current is the *sum* of electron and hole current. An exaggerated two-dimensional representation of the influence of the small electric field on the carrier velocity is shown in Fig. 2.13, illustrating the superposition of a drift velocity component upon the thermal velocity.

The force exerted by the field on an electron is $F = qE$. For a given field, this force is constant. From mechanics, it is known that when a constant force is applied to a particle, the particle is uniformly accelerated. Consequently, the drift velocity and hence the current would be expected to increase indefinitely under the influence of a constant electric field. This is in disagreement with the observed Ohm's law which specifies that, for a given field, the current "settles" at a steady-state value. Therefore, there must be "frictional" forces in a direction opposite to the accelerating force. A balance between the two forces must be reached rapidly so that the drift velocity settles at a constant average value. The motion of carriers in the crystal under the influence of a constant field can be compared with the fall of a steel ball in a viscous medium, such as heavy oil. While the constant force of gravity accelerates the steel ball, the frictional force that the viscous medium exerts on it slows it down. The friction increases as the velocity of the steel ball increases. Eventually, a point is reached where the force of gravity and the frictional forces cancel each other. At this point, there will be no net force exerted on the ball that

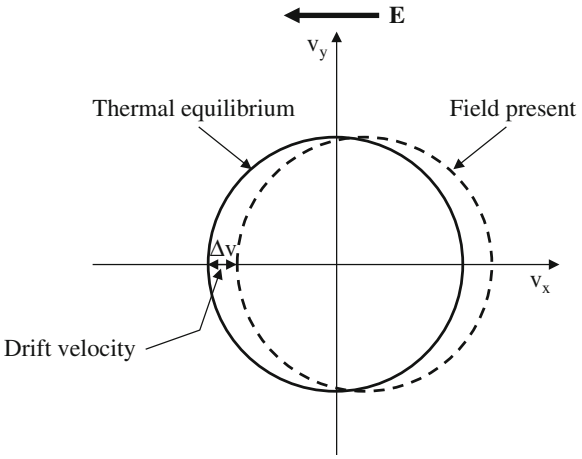

Fig. 2.13 Exaggerated two-dimensional representation of the influence of an electric field on the average electron velocity

now falls at a constant limiting velocity. The frictional forces produce a small rise in the temperature of the medium.

The electron drift velocity drift velocity can be expressed as

$$v_{dn} = \mu_n E \ \text{cm/s} \tag{2.28}$$

where μ_n is called the electron drift *mobility* in $\text{cm}^2/\text{V s}$ and, for simplicity, the average velocity is expressed as v_{dn} instead of $\langle v_{dn} \rangle$. Similarly, the drift velocity of holes is

$$v_{dp} = \mu_p E \ \text{cm/s} \tag{2.29}$$

where μ_p is the hole drift mobility in cm^2/Vs. The electron and hole mobility is an important parameter that plays a key role in device analysis. It is a measure of the ease with which the carriers move in the crystal and affects the performance of most devices.

Since electrons and holes move in opposite directions and their charges are of opposite polarity, both terms have the same sign, so that their sum constitutes the total current density:

$$j_n + j_p = q(v_{dn} n + v_{dp} p) = qE(\mu_n n + \mu_p p) \ \text{A/cm}^2 \tag{2.30}$$

The *conductivity* of the crystal is[3]

$$\sigma = \sigma_n + \sigma_p = q(\mu_n n + \mu_p p) \ \text{S/cm} \tag{2.31}$$

[3]The unit Siemens (S) is used for 1/Ω.

The *resistivity* is the inverse of conductivity and defined as:

$$\rho = \frac{1}{\sigma} = \frac{1}{q(\mu_n n + \mu_p p)} \quad \Omega\text{-cm} \tag{2.32}$$

If only donors at a concentration N_D are present, then ρ can be approximated as

$$\rho \cong \frac{1}{q\mu_n N_D} \quad \Omega\text{-cm} \tag{2.33}$$

Similarly, for only N_A

$$\rho \cong \frac{1}{q\mu_p N_A} \quad \Omega\text{-cm} \tag{2.34}$$

When both donors and acceptors are present at different concentrations, one type is totally compensated by the other. The *net* carrier concentration is approximated as the *difference* in concentration between the two impurities. As will be shown, the mobility would be affected by the both impurities.

(a) **Scattering Mechanisms**

The most important scattering mechanisms are *lattice scattering* and *ionized impurity* scattering. Other mechanisms, such as scattering by neutral atoms at low temperature, crystal-defect scattering, carrier–carrier scattering, are less important and will be discussed only where applicable.

The carrier mobility is limited by the rate of scattering events along its path. The scattering events are referred to as collisions. Between collisions, carriers gain energy from the electric field and transfer this energy to the atoms of the crystal upon collision. The energy transfer increases oscillations of crystal atoms and causes Joule heating. To simplify the analysis, it is assumed that upon collision, a carrier loses all the energy it gained from the external field and starts over again with a random velocity after a collision. In other words, after collision, the carrier has no memory of what happened before the collision.

Lattice Scattering In the presence of thermal vibrations, lattice atoms are compressed or pulled apart over small regions. Such displacements cause a disturbance to the periodic potential, deflecting carriers, and decreasing their mobility. This scattering mechanism is referred to as *lattice scattering*. The probability of collisions with the lattice increases with temperature because the number of vibrational modes and the amplitude of oscillations increase with temperature. As the oscillation amplitude increases, the cross-sectional area for collisions increases. Careful measurements show the following dependence for electron and hole mobility on temperature [10]

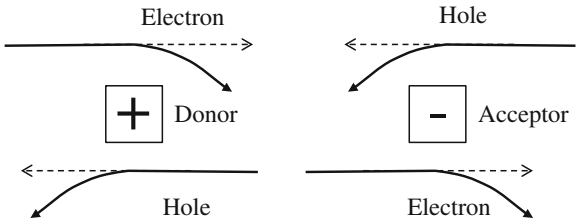

Fig. 2.14 Electron and hole collisions with dopant atoms causing Coulomb scattering

$$\mu_{\ln} \cong 2.10 \times 10^9 T^{-2.5} \ \text{cm}^2/\text{Vs} \tag{2.35}$$

$$\mu_{\text{lp}} \cong 2.34 \times 10^9 T^{-2.7} \ \text{cm}^2/\text{Vs} \tag{2.36}$$

where $\mu_{\ln}$ and μ_{lp} are the lattice-limited electron and hole mobilities, respectively.

Ionized Impurity Scattering A carrier moving in the vicinity of an ionized impurity is deflected by the Coulomb field of the ion. In their path near the ion, electrons are attracted by donors and repelled by acceptor while holes are attracted by acceptors and repelled by donors (Fig. 2.14).

When the crystal is doped with both donors and acceptors, both contribute to the net impurity scattering. A relation for the *ionized impurity scattering-limited mobility* as a function of temperature and ionized impurity concentration is adapted from [11] and simplified to

$$\mu_{\text{I}} = \frac{AT^{3/2}}{N_{\text{I}} \ln\left[1 + B\left(\frac{T^2}{N_{\text{I}}^{2/3}}\right)\right]} \ \text{cm}^2/\text{Vs} \tag{2.37}$$

where $A \cong 1.5 \times 10^{16}$ for electrons, $A \cong 7.3 \times 10^{15}$ for holes, and $B \cong 2.81 \times 10^6$ for electrons and holes [12].

The dependence of ionized impurity mobility on temperature can be intuitively understood by considering that elevating the temperature increases the carrier thermal velocity. This reduces the time the carrier spends in the vicinity of the ionized impurity and hence the deflection when it passes the ion, increasing the mobility.

Matthiessen's Rule In a simple model, the probabilities for scattering are additive, so that the lattice- and impurity-limited mobilities can be combined to give an effective mobility as

$$\frac{1}{\mu_{\text{eff}}} = \frac{1}{\mu_{\text{l}}} + \frac{1}{\mu_{\text{I}}} \tag{2.38}$$

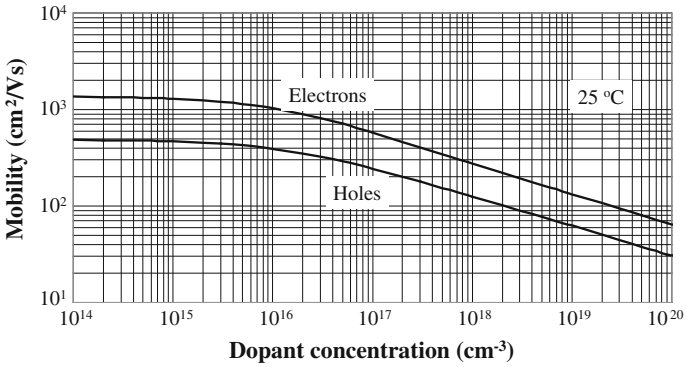

Fig. 2.15 Electron and hole mobility as a function of dopant concentration at 25 °C

The combination of different mobilities in the form of (2.38) is referred to as *Matthiessen's rule*. The calculated electron and hole mobility is plotted in Fig. 2.15 as a function of dopant concentration N at 25 °C. It should be noted, however, that there is appreciable spread in mobility data in the literature, particularly at higher concentrations [13–18].

Figure 2.16 compares the room temperature mobility as function of the concentration N using the following empirical expression derived from experimental data by [13] and modified slightly by [14–18]:

$$\mu_0 = \frac{\mu_{\max} - \mu_{\min}}{1 + (N/N_{\text{ref}})^{\alpha}} + \mu_{\min} \quad \text{cm}^2/\text{Vs} \tag{2.39}$$

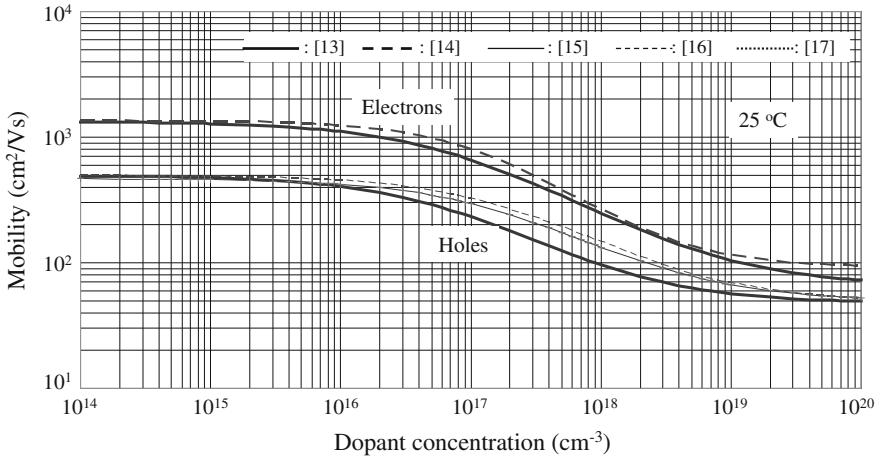

Fig. 2.16 Comparison of electron and hole mobility at 25 °C

Table 2.3 Values for parameters in (2.39)

Reference	Electrons				Holes			
	μ_{max}	μ_{min}	N_{Ref}	α	μ_{max}	μ_{min}	N_{Ref}	α
[13]	1330	65	8.5×10^{16}	0.72	495	47.7	6.3×10^{16}	0.76
[14]	1360	92	1.3×10^{17}	0.91				
[15]					495	47.7	1.9×10^{17}	0.76
[16]					468	49.7	1.6×10^{17}	0.70
[17]	1330.1	88.3	1.295×10^{17}	0.891	461.2	54.3	2.35×10^{17}	0.88

The parameter values for μ_{max}, μ_{min}, (cm^2/Vs), N_{ref} (cm^{-3}) and α are shown in Table 2.3. N is the total doping concentration.

The temperature dependence of mobility is shown in Fig. 2.17 for $N = 10^{15}$, 10^{16}, 10^{17}, and 10^{18} cm^{-3}.

Substituting the effective mobility in (2.33) and (2.34) provides a good approximation of resistivity as a function of impurity concentration and temperature. Figure 2.18 compares the resistivity obtained from calculations (dashed lines) with measured results from [19, 20] (solid lines).

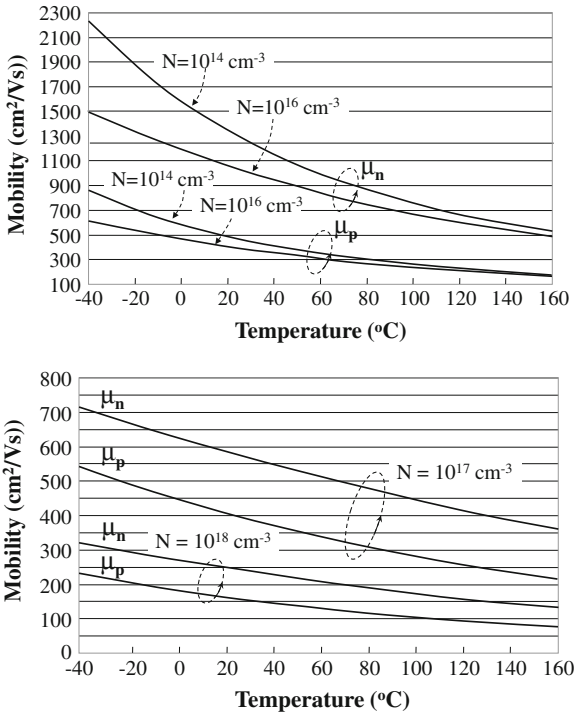

Fig. 2.17 Temperature dependence of electron and hole mobilities for four different concentrations [18]

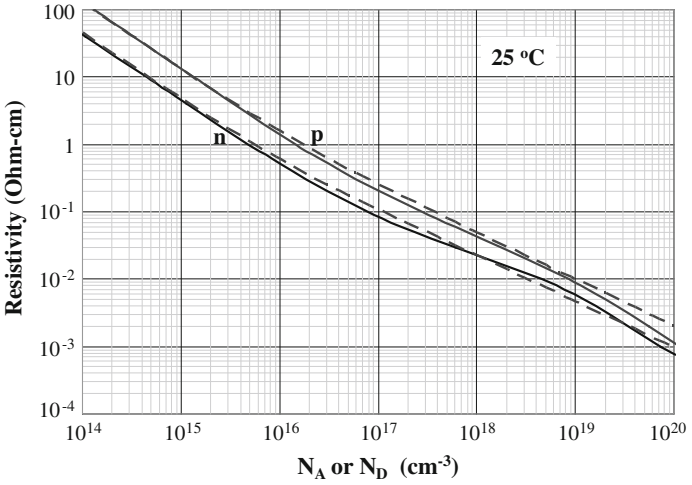

Fig. 2.18 Resistivity versus impurity concentration at 25 °C. *Solid lines* measured resistivity [19, 20]; *dashed lines* calculated

2.5.2 Carrier Transport by Drift—High Field

The drift velocity of electrons and holes in silicon is shown as a function of electric field in Fig. 2.19. The plots are constructed from an empirical relation that constitutes a best fit to measured data at 27 °C [13]:

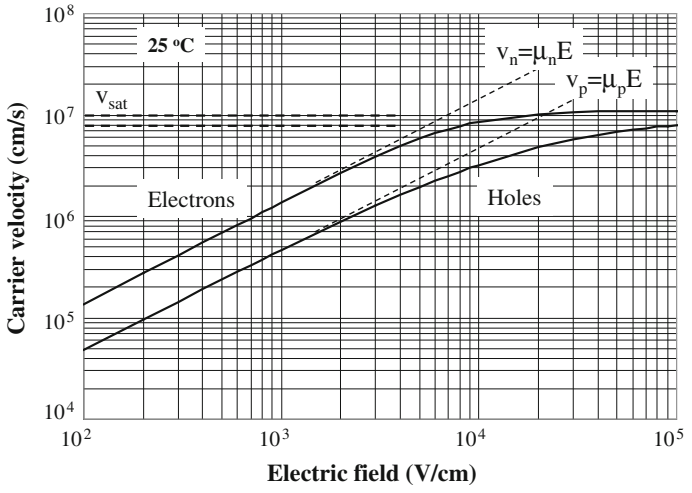

Fig. 2.19 Carrier drift velocity versus electric field [13]

Table 2.4 Values for fitting parameters in (2.40a, b)

	E_{sat} (V/cm)	v_{sat} (cm/s)	β
Electrons	8×10^3	1.1×10^7	2
Holes	1.95×10^4	9.5×10^6	1

$$v_d \approx v_{sat} \frac{E/E_{sat}}{\left[1 + (E/E_{sat})^{\beta}\right]^{\frac{1}{\beta}}} \text{ cm/s} \tag{2.40a}$$

The fitting parameters are summarized in Table 2.4 for *high-resistivity* silicon [13]. The mobility field dependence is approximated as

$$\mu \approx \frac{\mu_0}{\left[1 + (E/E_{sat})^{\beta}\right]^{\frac{1}{\beta}}} \text{ cm}^2/\text{Vs} \tag{2.40b}$$

where μ_0 is the low-field mobility given by (2.39). Treating v_{sat} as constant, $E_{sat} = v_{sat}/m_0$, dependent on doping [13].

At a field less than about 5×10^3 V/cm, the drift velocity is proportional to electric field. The proportionality factor is the mobility, as defined in (2.28) and (2.29). In the range between 5×10^3 and 5×10^4 V/cm, the mobility decreases so that the dependence of drift velocity on electric field digresses from linearity. As the field increases above $\sim 5 \times 10^4$ V/cm, the drift velocity begins to saturate to a value v_{sat} close to the thermal velocity of 10^7 cm/s (Fig. 2.19).

The departure from linearity and the saturation of velocity can be qualitatively explained in terms of different vibration mechanisms in the crystal. Oscillation of atoms in the crystal can be visualized by comparing the crystal lattice with a three-dimensional periodic set of mass points, spaced a distance a apart and each attached to six adjacent identical springs [4, 6]. In such as system, a multitude of standing waves of different wavelengths can be generated at a frequency that depends on the force constant of the springs, with nodes appearing at the system boundaries. In a crystal, there are two modes of oscillation of different frequencies associated with each wavelength, one in which two atoms in a unit cell oscillate in phase (Fig. 2.20a), and the other where they move out of phase (Fig. 2.20b).

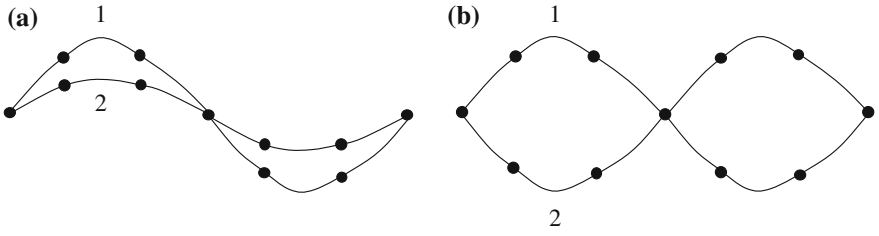

Fig. 2.20 Schematic representation of oscillation modes in a crystal. **a** Atoms in phase, acoustical phonons. **b** Atoms out of phase, optical phonons

As in the case of electrons and photons, an oscillation in a crystal has a frequency v and an associated quantum of energy $E = hv$ called a *phonon* (h is Planck's constant). When atoms oscillate approximately in phase, as illustrated in Fig. 2.20a, the relative displacement between atoms is small and the restoring force is small. Therefore, the frequency associated with such oscillations is small and the phonon energy is small. The wave propagation corresponds to ordinary sound waves in the crystal so the quanta of energy are referred to as *acoustical phonons*. When the atoms move in approximately opposite directions, as shown in Fig. 2.20b, they are characterized by higher frequencies, hence higher energies than in (a), because of the large restoring force associated with the opposite motion of atoms. This mode of oscillation is called optical and the associated quanta of energy called *optical phonons* because, if the atoms were oppositely charged, such as in NaCl crystals, the vibrations would give rise to oscillating electric dipole moments and electromagnetic radiation is emitted or absorbed during the process [4, 6].

When the field is smaller than about 5×10^3 V/cm, the carriers interact predominantly with acoustical phonons because their kinetic energy is not sufficiently high to generate optical phonons. When the field is varied in this range, the carriers rapidly exchange energy with acoustical phonons and reach a new steady-state average velocity that is proportional to the field, i.e., $dv_d/dE = \text{constant} = \mu_0$, where μ_0 is the low-field mobility defined in (2.28) and (2.29). In this region, the carrier temperature does not increase appreciably over the crystal temperature.

As the field increases above approximately 5×10^3 V/cm, the carrier energy increases to a point where the probability for generation of optical phonons becomes significant. An increasing fraction of energy gained from the electric field is now lost by generation of optical phonons and the rate of change in drift velocity decreases, i.e., $dv_d/d\boldsymbol{E}$ decreases. Therefore, as the field increases above a "critical level," the mobility begins to decrease below its low-field value ($\mu < \mu_0$). In the limit, the carriers lose all incremental energy gained from the field to the crystal and their velocity does not further increase, i.e., the velocity reaches a nearly constant saturation velocity v_{sat}. In this range, the energy imparted by the electric field is transferred to the crystal and increases the number of carriers at velocity saturation instead of increasing the carrier drift velocity. In the range above approximately 5×10^4 V/cm, the carrier temperature increases above the lattice temperature and carriers are said to be *hot carriers*. Important hot-carrier effects are discussed in the following sections.

2.5.3 Carrier Transport by Diffusion

Free particles in any system are in constant random thermal motion. When the carrier concentration is uniform and no external disturbance is present, as many carriers move, on the average, in one direction as in the other and the net number of carriers passing through a unit area per unit time, the carrier flux, in any direction is zero. In the presence of a concentration gradient, however, the probability for a

carrier to move in one direction can be the same everywhere but there are more carriers in a region of high concentration than outside that region. Hence, there will be a net flux of carriers moving outward from that region. The flow of carriers in response to a concentration gradient is referred to as diffusion. It is the same process that spreads smoke in air. In a semiconductor, electrons and holes are carriers of charge and their transport by diffusion gives rise to diffusion current.

A thorough analysis shows that the electron diffusion current density in one dimension is

$$j_{\mathrm{n(dif)}} = qD_{\mathrm{n}} \frac{\mathrm{d}n(x)}{\mathrm{d}x} \quad \mathrm{A/cm^2} \tag{2.41}$$

where q is the charge of an electron (-1.6×10^{-19} C), D_{n} is the electron diffusivity ($\mathrm{cm^2/s}$), and $\mathrm{d}n(x)/\mathrm{d}x$ is the gradient in electron concentration. For electrons flowing in the positive x-direction, $\mathrm{d}n(x)/\mathrm{d}x$ is negative because it points in the direction of decreasing concentration. Since the electron charge q is negative, j_{n} is positive.

Similarly, for holes moving in the x-direction, the hole current density in one dimension is

$$j_{\mathrm{p(dif)}} = -qD_{\mathrm{p}} \frac{\mathrm{d}p(x)}{\mathrm{d}x} \quad \mathrm{A/cm^2} \tag{2.42}$$

where D_{p} is the diffusivity of holes, and $\mathrm{d}p(x)/\mathrm{d}x$ is the gradient in hole concentration. In this case, the electron and hole currents are in opposite directions because of their opposite charge. The total diffusion current density in the x-direction is then

$$j_{\mathrm{(dif)}} = j_{\mathrm{n(dif)}} + j_{\mathrm{p(dif)}} = q\left(D_{\mathrm{n}} \frac{\mathrm{d}n}{\mathrm{d}x} - D_{\mathrm{p}} \frac{\mathrm{d}p}{\mathrm{d}x}\right) \quad \mathrm{A/cm^2} \tag{2.43}$$

The average carrier velocity in the x-direction can be obtained from (2.26), (2.41), and (2.42) as

$$v_{\mathrm{n(dif)}} = D_{\mathrm{n}} \frac{\mathrm{d}n}{\mathrm{d}x} \frac{1}{n} \quad \mathrm{cm/s} \tag{2.44}$$

$$v_{\mathrm{p(dif)}} = -D_{\mathrm{p}} \frac{\mathrm{d}p}{\mathrm{d}x} \frac{1}{p} \quad \mathrm{cm/s} \tag{2.45}$$

2.5.4 Total Drift and Diffusion Current Density

Both drift and diffusion contribute in varying degrees to the total current density. The two mechanisms are typically independent events and can be combined to give the total current density. In one dimension, this is for electrons

$$j_n = j_{n(drift)} + j_{n(dif)} = q\mu_n nE + qD_n \frac{dn}{dx} \quad A/cm^2 \tag{2.46}$$

and for holes

$$j_p = j_{p(drift)} + j_{p(dif)} = q\mu_p pE - qD_p \frac{dp}{dx} \quad A/cm^2 \tag{2.47}$$

The drift terms in the above equations have the same algebraic sign because the electric field produces conventional current in the same direction for opposite charged particles.

2.5.5 Non-uniform Doping Concentration

So far, only uniformly doped silicon was considered. In most device regions, however, the dopant concentrations are non-uniform. In this case, the bulk Fermi potential ϕ_b in (2.25a, b) becomes a function of position in the doped region, as illustrated in Fig. 2.21 in one dimension for N-type silicon at thermal equilibrium. Since the crystal is at thermal equilibrium, the net current in any direction is zero. When there is no current in any region, the Fermi level is shown flat. For not too high concentrations, the energy gap remains constant but the bands are bent.

The *electrostatic potential* with respect to the arbitrary reference energy level E_{ref} parallel to E_F is

$$V(x) = -\frac{E_C(x) - E_{ref}}{q} \quad V \tag{2.48}$$

Because of the dopant non-uniformity, a *built-in field* $\boldsymbol{E}$ exists, given by[4]

$$E = -\frac{d\phi_b}{dx} = \frac{1}{q}\frac{dE_C}{dx} = \frac{1}{q}\frac{dE_V}{dx} = \frac{1}{q}\frac{dE_i}{dx} \quad V/cm \tag{2.49}$$

This built-in field induces a drift current component that at thermal equilibrium is exactly balanced by a diffusion current component in the opposite direction. The balance can be visualized by considering that the concentration gradient in Fig. 2.21 causes electrons to diffuse from right to left but as they diffuse, electrons leave uncompensated positively charged donor ions behind creating a positive field that forces electrons to drift back from left to right. At equilibrium, the drift current is exactly balanced by the diffusion current and the net current is zero. In this case, (2.46) and (2.47) reduce to

[4]Bold $\boldsymbol{E}$ is used for electric field to distinguish it from energy E.

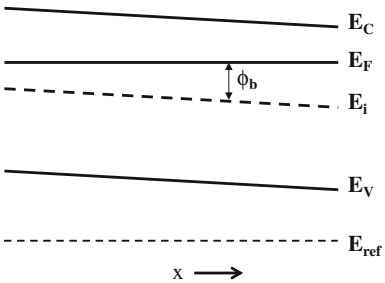

Fig. 2.21 Simplified band diagram for non-uniformly doped N-type silicon at thermal equilibrium. The concentration drops from right to left. E_{ref} is a convenient, arbitrary reference energy level

$$q\mu_{\text{n}}\overline{n}E = -qD_{\text{n}}\frac{\text{d}\overline{n}}{\text{d}x} \tag{2.50}$$

$$q\mu_{\text{p}}\overline{p}E = qD_{\text{p}}\frac{\text{d}\overline{p}}{\text{d}x} \tag{2.51}$$

where $\bar{n}$ and $\bar{p}$ are the position-dependent equilibrium electron and hole concentrations.

2.5.6 Einstein Relation

In the above equations, the carrier mobility and diffusivity, D, are both controlled by scattering mechanisms in the crystal. They are connected by an equation known as the *Einstein's relation* [1.1, 1.4]:

$$D_{\text{n}} = \mu_{\text{n}}\frac{kT}{q} \quad \text{cm}^2/\text{s} \tag{2.52}$$

$$D_{\text{p}} = \mu_{\text{p}}\frac{kT}{q} \quad \text{cm}^2/\text{s} \tag{2.53}$$

Substituting the above expressions for the electron and hole diffusivity, D_{n} and D_{p} in (2.50) and (2.51) gives important relations between the built-in field and the gradient in dopant concentration:

$$E = -\frac{1}{\overline{n}}\frac{kT}{q}\frac{\text{d}\overline{n}}{\text{d}x} = -\frac{1}{N_{\text{D}}}\frac{kT}{q}\frac{\text{d}N_{\text{D}}}{\text{d}x} \quad \text{V/cm} \tag{2.54}$$

$$E = \frac{1}{\overline{p}} \frac{kT}{q} \frac{d\overline{p}}{dx} = \frac{1}{N_A} \frac{kT}{q} \frac{dN_A}{dx} \quad \text{V/cm} \tag{2.55}$$

2.6 Non-equilibrium Conditions

When the crystal is at thermal equilibrium, the rate of thermally generated electron–hole pairs in a volume element is balanced by a statistically equal rate of electron–hole pair recombination. In this case,

$$\overline{pn} = n_i^2 \quad \text{cm}^{-6}$$

A non-equilibrium condition occurs when excess carriers are generated by an external stimulus, such as light, whereby

$$pn > n_i^2 \tag{2.56}$$

When the stimulus is removed, the system tends to restore equilibrium by an excess recombination over generation.

In situations where the electron and hole concentrations are reduced below their equilibrium values,

$$pn < n_i^2 \tag{2.57}$$

In this case, there will be an excess in thermal generation over recombination. Such situations are found in, e.g., reverse-biased pn junctions, as discussed in Chap. 3. This section discusses the mechanisms involved in recombination processes in the silicon bulk.

2.6.1 Carrier Lifetime

Excess carriers can be created, for example, by illuminating the crystal with photons of energy ≥ E_g, or by forward biasing a pn junction as described in the next chapter. In the case of illumination, if the intensity of light is kept constant, a non-equilibrium steady-state condition is achieved where the electron and hole concentrations are larger than their thermal equilibrium values and a new rate of generation is balanced by a new rate of recombination. Let Δp and Δn be the excess carrier concentrations. The steady-state concentrations are given as follows:

$$p = \overline{p} + \Delta p \tag{2.58}$$

$$n = \overline{n} + \Delta n \tag{2.59}$$

Because electrons and holes are generated or annihilated in pairs, $\Delta p = \Delta n$ and the crystal as a whole remains neutral. An increase in the minority carriers above thermal equilibrium concentration is called *minority-carrier injection*. Consider, for example, a P-type silicon sample with $N_A = 10^{16}$ cm^{-3}. At room temperature, where nearly complete ionization occurs, the thermal equilibrium majority hole concentration is about 10^{16} cm^{-3} and the minority electron concentration is about 2×10^4 cm^{-3}. If the sample is illuminated with light of intensity that caused an increase in the carrier concentrations by, e.g., $\Delta n = \Delta p = 10^{12}$ cm^{-3}, the fractional increase in majority hole concentration is negligibly small, $\Delta p/\overline{p} = 0.01\,\%$, while the minority electron concentration increases by over seven orders of magnitude. When the increase in carrier concentration is small compared to the *majority* thermal equilibrium concentration, the injection is referred to as *low-level injection*.

The time-dependence of the recombination process is characterized by a *carrier lifetime*, which is the time for the excess concentration to decay by 1/e of its starting value. If by some means excess majority carriers could be created in silicon without a simultaneous increase in minority carriers and the stimulus instantaneously removed, the excess majority carriers would dissipate in a very short time, typically 10^{-12}–10^{-11} s (see also Problem 1.8). In comparison, excess minority carriers have a much longer lifetime, even as long as seconds. Because of the required neutrality, however, excess majority carriers will remain present as long as excess minority carriers are present. It is the minority-carrier lifetime that plays a key role in device applications. At low-level injection, the rate of recombination of excess minority carriers is typically proportional to their concentration

$$\frac{\mathrm{d}\Delta n(t)}{\mathrm{d}t} = -C\Delta n(t) \quad \mathrm{cm}^{-3} \tag{2.60}$$

where C is a constant. The decay of excess carriers can then be expressed as

$$\Delta n(t) = \Delta n_0 \mathrm{e}^{-t/\tau} \quad \mathrm{cm}^{-3} \tag{2.61}$$

In Eq. (2.61), Δn_0 is the excess minority concentration at the time $t = t_0$, e.g., where the stimulus was stopped, and t the average minority-carrier lifetime, i.e., the time where the excess minority-carrier concentration has decayed to 1/e of its value at the time $t = 0$.

The minority-carrier lifetime is determined by the rate at which excess electrons and holes recombine, or annihilate. Recombination processes are discussed next.

(a) Direct Band-to-Band Transitions

Band-to-band recombination is a direct transition of an electron from the bottom of the conduction band to the top of the valence band whereby an electron–hole pair is

annihilated. The rate of this recombination process is expected to be proportional to the electron and hole concentrations. When such a transition occurs, a photon of energy equal to the bandgap is emitted. The probability for such transitions is high in direct bandgap semiconductors, such as GaAs, where electrons at E_C and holes at E_V have the same *momentum*. The actual band diagram of silicon is more complex than in Fig. 2.5. It shows that silicon is an indirect bandgap semiconductor where free electrons at E_C have higher momentum than holes at E_V. Because energy and momentum must be conserved during transitions between E_C and E_V, and the electron cannot lose its momentum at once, the transitions become unlikely without assistance of other mechanisms that absorb the excess momentum. The energy is transferred in steps to the crystal instead.

(b) **Transitions Involving Intermediate States**

The minority-carrier lifetime in silicon crystals is found to be considerably smaller than the lifetime expected from direct band-to-band transition probability. For low to moderately doped silicon, this can be explained by the presence of recombination centers in the crystal [21, 22]. These are energy states distributed within the bandgap and created by impurities other than dopants, such as heavy metals. The minority carrier can thus orbit for a short time around the center with an energy intermediate between the valence and conduction band edges and give its energy to the crystal in a two- or multiple-step process, transferring to the crystal a smaller amount of energy in each step. The different transitions through intermediate steps are shown schematically in Fig. 2.22 [23]. The centers are shown at mid-gap for simplicity, but in real crystals this is not the case as can be seen from Fig. 2.23 which shows the energy levels associated with a number of different impurity atoms [24].

From statistical analysis, it can be shown that the efficiency of a center to act as a recombination or generation site is at maximum when its energy level is exactly at mid-gap [21–24]. By assuming an effective density of recombination-generation

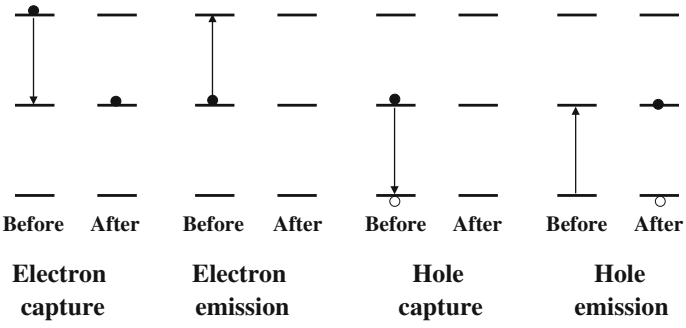

Fig. 2.22 Schematic model for transitions through intermediate states. *Arrows* represent direction of electron transition (adapted from [23])

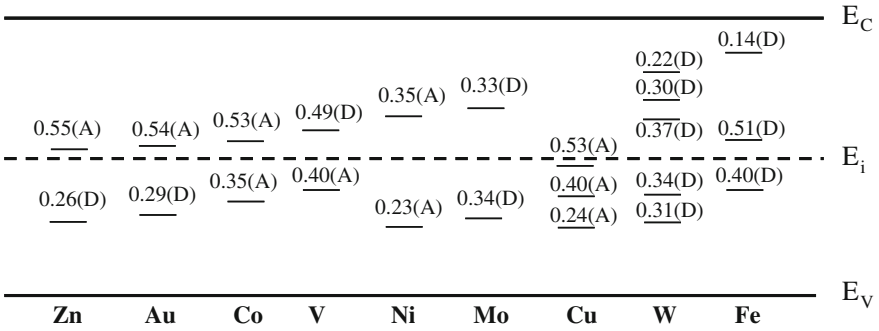

Fig. 2.23 Measured ionization energies for selected deep-level impurities in silicon. *Levels above* E_i are referenced to E_C and *levels below* E_i are referenced to E_V (adapted from [24])

centers, N_t, located at mid-gap, the rate of recombination (and generation) of minority carriers can be approximated as

$$U = \sigma v_{th} N_t \Delta n \quad \text{(electrons)} \quad \text{cm}^{-3}/\text{s} \tag{2.62}$$

$$U = \sigma v_{th} N_t \Delta p \quad \text{(holes)} \quad \text{cm}^{-3}/\text{s} \tag{2.63}$$

U is the recombination rate (cm^{-3}/s), σ is the capture cross section, assumed to be the same for electrons and holes ($\cong 10^{-15}$ cm^2), v_{th} is the thermal velocity ($\cong 10^7$ cm/s), and N_t is the effective density of recombination-generation centers (cm^{-3}).

The density of recombination-generation centers depends on the crystal properties and processing conditions. In good crystals, N_t ranges typically from 10^{10} to 10^{12} cm^{-3}. In case of N-type silicon, the hole lifetime can be approximated as

$$\tau_{SRH} = \frac{\Delta p}{U} = \frac{1}{\sigma v_{th} N_t} \text{ s} \tag{2.64}$$

A similar relation is found for minority-carrier electrons. Generation-recombination through intermediate states is referred to as the Shockley-Read-Hall (SRH) process [21, 24].

(c) Auger Recombination

Another mechanism for minority carriers to recombine is to transfer its excess energy *and* momentum to a third carrier available in its vicinity. This recombination process is known as *Auger recombination* and illustrated in Fig. 2.24 [25, 26]. Auger recombination requires at least two free majority carriers in the vicinity of the minority carrier, one with which the minority carrier recombines and another to which it gives the resulting energy and momentum. Auger recombination becomes significant, even dominates, in heavily doped regions, in the range 10^{19}–10^{21} cm^{-3},

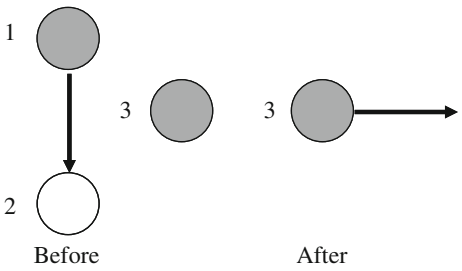

Fig. 2.24 Auger recombination. Electron (*1*) recombines with hole (*2*). An electron (*3*) in the vicinity absorbs the excess energy and momentum

where free majority carriers are abundant. The Auger recombination lifetime is approximated for holes in N-type silicon as

$$\tau_{\mathrm{Ap}} \cong \frac{1}{r_{\mathrm{Ap}} n^2} \ \mathrm{s} \tag{2.65}$$

and for electrons in P-type silicon as

$$\tau_{\mathrm{An}} \cong \frac{1}{r_{\mathrm{An}} p^2} \ \mathrm{s} \tag{2.66}$$

where n and p are, respectively, the majority carrier electron and hole concentrations, and r_{Ap} and r_{An} are the Auger recombination rates found at room temperature as [25]

$$r_{\mathrm{Ap}} = 9.9 \times 10^{-32} \ \mathrm{cm}^6/\mathrm{s} \tag{2.67}$$

$$r_{\mathrm{An}} = 2.8 \times 10^{-31} \ \mathrm{cm}^6/\mathrm{s} \tag{2.68}$$

In the presence of Auger recombination, the effective carrier lifetime is limited by a combination of SRH and Auger recombination mechanisms as

$$\frac{1}{\tau_{\mathrm{p-eff}}} = \frac{1}{\tau_{\mathrm{SRH}}} + \frac{1}{\tau_{\mathrm{Ap}}} \ \mathrm{s}^{-1} \tag{2.69}$$

$$\frac{1}{\tau_{\mathrm{n-eff}}} = \frac{1}{\tau_{\mathrm{SRH}}} + \frac{1}{\tau_{\mathrm{An}}} \ \mathrm{s}^{-1} \tag{2.70}$$

where t_{SRH} is the SRH lifetime.

(d) Diffusion Length

Continuity for each type of carrier relates the net rate of change of carriers within a volume element to the generation, recombination, and the flow of carriers into or

out of the volume element. Consider, for example, N-type silicon in which electron–hole pairs are generated, e.g., by light in a volume region of the crystal. The one-dimensional continuity relation for minority-carrier holes is

$$\frac{\mathrm{d}p}{\mathrm{d}t} = G - \frac{\Delta p}{\tau_\mathrm{p}} + \frac{1}{q}\frac{\mathrm{d}j_\mathrm{p}}{\mathrm{d}x} \quad \mathrm{cm}^{-3}\,\mathrm{s}^{-1} \tag{2.71}$$

where the three terms represent generation, recombination, and current divergence, respectively. Under steady-state conditions, the rate of change in the minority-carrier concentration is

$$\frac{\mathrm{d}p}{\mathrm{d}t} = \frac{\mathrm{d}\Delta p}{\mathrm{d}t} = 0 \tag{2.72}$$

and

$$\frac{1}{q}\frac{\mathrm{d}j_\mathrm{p}}{\mathrm{d}x} = G - \frac{\Delta p}{\tau_\mathrm{p}} \quad \mathrm{cm}^{-3}\,\mathrm{s}^{-1} \tag{2.73}$$

If a point is chosen far away from the source of generation, $G = 0$ and

$$\frac{1}{q}\frac{\mathrm{d}j_\mathrm{p}}{\mathrm{d}x} = -\frac{\Delta p}{\tau_\mathrm{p}} \quad \mathrm{cm}^{-3}\,\mathrm{s}^{-1} \tag{2.74}$$

The current density j_p has a drift and diffusion component. Since holes are minority carriers, they do not contribute appreciably to the total drift current. In this case, only the diffusion component of hole current is significant and can be approximated as

$$j_\mathrm{p} = -qD_\mathrm{p}\frac{\mathrm{d}\Delta p}{\mathrm{d}x} \quad \mathrm{A/cm}^2 \tag{2.75}$$

Substituting the above expression in (2.74) gives

$$\frac{\mathrm{d}^2\Delta p}{\mathrm{d}x^2} = \frac{\Delta p}{D_\mathrm{p}\tau_\mathrm{p}} \tag{2.76}$$

For regions very far away from the source of generation, one can set $x = \infty$ and $\Delta p = 0$. The solution of (2.76) with this boundary condition has the form

$$\Delta p = \Delta p_0 \mathrm{e}^{-x/\sqrt{D_\mathrm{p}\tau_\mathrm{p}}} \quad \mathrm{cm}^{-3} \tag{2.77}$$

where Δp_0 is the excess hole concentration at the point of reference $x = x_0$. The square root term in the exponent is the average distance at which the excess carrier

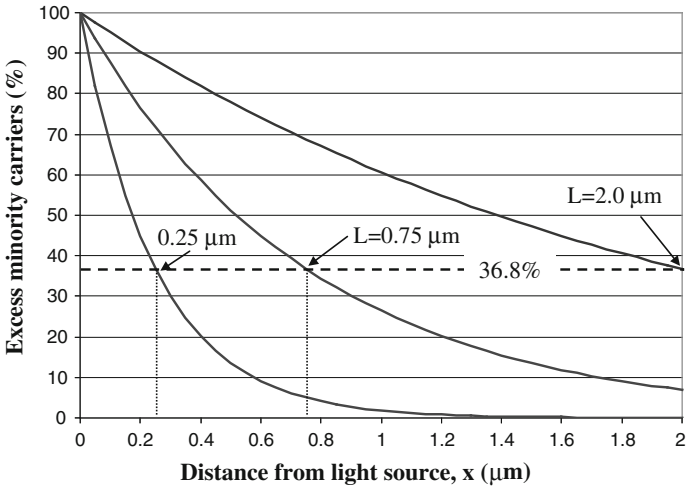

Fig. 2.25 Excess minority-carrier concentration versus distance for three diffusion lengths L

concentration has decayed to 1/e of its value at the reference point $x = x_0$ (Fig. 2.25). This distance is referred to as the hole *diffusion length*, L_p, where

$$L_p = \sqrt{D_p \tau_p} \text{ cm} \tag{2.78}$$

Similarly, for minority-carrier electrons

$$L_n = \sqrt{D_n \tau_n} \text{ cm} \tag{2.79}$$

The minority-carrier diffusion length depends mainly on its lifetime since the diffusivity, D, which is proportional to μ (2.52), does not vary widely within a doped crystal, yet the lifetime may vary orders of magnitude depending on the concentration of lifetime-killing (i.e., SRH) impurities.

Example 2.6 The electron lifetime in a 10 Ω-cm P-type silicon crystal is 0.5 ms at 25 °C. Estimate (a) The effective density of recombination centers and (b) The electron diffusion length.

Solution

(a) Electrons are minority carriers. Assuming a thermal velocity $v_{th} = 10^7$ cm/s and a capture cross section $s_n = 10^{-15}$ cm^2, the effective density of recombination centers is found from (2.63) as

$$N_t \approx \frac{1}{5 \times 10^{-4} \times 10^7 \times 10^{-15}} = 2 \times 10^{11} \text{ cm}^{-3}$$

(b) From Fig. 2.17, the acceptor concentration in a 10 Ω-cm silicon crystal is approximated as 1.2×10^{15} cm^{-3}. The electron mobility at this concentration is estimated from Fig. 2.15 as 1300 cm^2/Vs. The electron diffusivity is found from (2.52) as

$$D_n = \mu_n \frac{kT}{q} = 1300 \times 0.0257 = 33.4 \text{ cm}^2/\text{s}$$

Substituting the values in (2.76) gives the electron diffusion length

$$L_n = \sqrt{33.4 \times 5 \times 10^{-4}} \approx 0.13 \text{ cm}$$

Problems

1. A region in silicon is uniformly doped with 10^{18} boron atoms/cm^3. Assume the region to have a length of 50 nm, a width of 1 mm, and a thickness of 100 nm and estimate the number of boron atoms in the region. What is the average distance between two boron atoms?
2. What is the percentage of covalent bonds broken in pure silicon at 100 °C?
3. Silicon is doped with 10^{16} cm^{-3} phosphorus atoms/cm^3. At what temperature would the hole concentration be equal to 10 % of the ionized impurity concentration?
4. Silicon is doped with 10^{15} cm^{-3} phosphorus atoms/cm^3. At what temperature is $n = 0.9\ N_D$? (Use the Fermi–Dirac distribution function).
5. Calculate the conductivity of pure silicon at 25 °C, and for silicon doped with 10^{16} boron atoms/cm^3 plus 10^{16} arsenic atoms/cm^3.
6. The sheet resistance R_S of a film is defined as the resistance measured between two opposite sides of a square of the film. Show that for a film thickness t, the sheet resistance along the surface is
$$R_S = \frac{\overline{\rho}}{t}$$
where $\bar{\rho}$ is the average film resistivity.
7. The boron profile in a 0.1-μm-deep transistor region in silicon can be approximated by an exponential function of the form
$$N_A(x) = 5 \times 10^{18} e^{-90x}$$
where x is the depth in μm from the surface.
   (a) Calculate the average sheet resistance at 25 °C.
   (b) Show that the built-in field is constant in the region.
8. An N-type layer in silicon is formed by phosphorus ion-implantation into a 10 Ω-cm substrate. The phosphorus profile after activation can be approximated by a Gaussian distribution as

$$N_D(x) = \frac{\phi}{\Delta R_p \sqrt{2\pi}} e^{-(x-R_p)^2/2\Delta R_p^2}$$

where ϕ is the implanted dose in atoms/cm^2, R_p is the projected range, and ΔR_p is the straggle. Assume full ionization and rind the sheet resistance of the layer at 25 °C for $\phi = 5 \times 10^{12}$ cm^{-2}, $R_p = 0.13$ μm, and $\Delta R_p = 0.05$ μm.

9. Consider a homogeneous conductor of conductivity σ and dielectric permittivity ε. Assume a mobile charge concentration

$$\rho(x, y, z, t = 0)$$

in space at a time $t = 0$.

The following relations stem from electromagnetism:

$$\nabla \cdot D = \rho; \quad D = \varepsilon E; \quad J = \sigma E; \quad \nabla \cdot J = -\frac{d\rho}{dt}$$

Show from these facts that

$$\rho(x, y, z, t) = \rho(x, y, z, t = 0) e^{-t/(\varepsilon/\sigma)}$$

Interpret this result to show that mobile charge cannot remain in the bulk of uniform conducting material, but must accumulate at surfaces of discontinuity, or other places of non-uniformity. Find the value of the "dielectric relaxation time" ε/σ for a typical metal and for P-type silicon with $N_A = 10^{15}$ cm^{-3} and N-type silicon with $N_D = 10^{17}$ cm^{-3} [3].

10. An N-type region in silicon is uniformly doped with arsenic at a concentration $N_D = 10^{20}$ cm^{-3}. Assume full ionization and an effective density of recombination centers $N_t = 10^{12}$ cm^{-3} and estimate the hole diffusion length in the region at 25 °C.

References

1. C. Kittel, *Introduction to Solid-State Physics*, John Wiley and Sons, New York, 1968.
2. W. Shockley, *Electrons and Holes in Semiconductors*, D. Van Nostrand Company, 1950
3. R. B. Adler, A. C. Smith and R. L. Longini, *Introduction to Semiconductor Physics,* Semiconductor Electronics Education Committee, Vol. 1, J. Wiley & Sons, 1964.
4. W. Finkelburg, *Einfuehrung in die Atomphysik*, Springer Verlag, 1958.
5. J. L. Moll, *Physics of Semiconductors*, McGraw-Hill, 1964.
6. A. J. Dekker, *Solid State Physics*, Prentice-Hall, 1965.
7. F. J. Morin and J. P. Maita, "Electrical properties of silicon containing arsenic and boron," Phys. Rev., **96** (1), 28-35, 1954.
8. E. M. Conwell, "Properties of silicon and germanium," Part II, Proc. IRE, **46** (6), 1281-1300, 1958.
9. B. El-Kareh, *Fundamentals of Semiconductor Processing Technologies*, Kluwer Academic Press, 1995.

10. G. W. Ludwig and R. L Watters, “Drift and conductivity mobility in silicon,” Phys. Rev., **101** (6), 1699-1701, 1956.
11. E. M. Conwell and V. F. Weisskopf, “Theory of impurity scattering in semiconductors,” Phys. Rev., **77** (3), 388-390, 1950.
12. B. El-Kareh, *Silicon Devices and Process Integration, Deep Submicron and Nano-scale Technologies*, Springer, 2009.
13. D. M. Caughey and R. E. Thomas, “Carrier mobilities in silicon empirically related to doping and field,” Proceeding of the IEEE, **55** (12), 2192-2193, 1967.
14. G. Baccarani and P. Ostoja, “Electron mobility empirically related to phosphorus concentration in silicon,” Solid-State Electronics, **18** (6), 579-580, 1975.
15. D. A. Antoniadis, A. G. Gonzalez, and R. W. Dutton, “Boron in near intrinsic <100> and <111> silicon under inert and oxidizing ambients – diffusion and segregation,” J. Electrochem. Soc.: Solid-State Science and Technology, **125** (5), 813-819, 1978.
16. S. Wagner, “Diffusion of boron from shallow ion implants in silicon,” J. Electrochem. Soc.: Solid-State Science and Technology, **119** (1), 1570-1576, 1972.
17. N. D. Arora, J. R. Hauser, and D. J. Roulston, “Electron and hole mobilities in silicon as a function of concentration and temperature,” IEEE Trans. Electron Dev., ED-**29** (2), 292-295, 1982.
18. W.W. Gartner, “Temperature dependence of junction transistor parameters,” Proc. of the IRE, **45** (5), 662-680, 1957.
19. J. C. Irvin, “Resistivity of bulk silicon and of diffused layers in silicon,” Bell Syst. Tech. J., 41, 387-410, 1962.
20. W. R. Thurber,R. L. Mattis, Y. M. Liu, and J. J. Filliban, “Resistivity-dopant density relationship for phosphorus-doped silicon,” J. Electrochem. Soc.: Solid-State Science and Technology, **12**, (8), 1807, 1980.
21. W. Shockley and W. T. Read, “Statistics of the recombination of holes and electrons,” Phys. Rev., **87** (5), 835-842, 1952.
22. R. N. Hall, “Electron-hole recombination in germanium,” Phys. Rev., **87** (2), 387, 1952.
23. A. S. Grove, *Physics and Technology of Semiconductor Devices*, John Wiley and Sons, 1967.
24. S. M. Sze, *Physics of Semiconductor Devices*, John Wiley and Sons, 1981.
25. J. Dziewior and W. Schmid, “Auger recombination coefficients for highly doped and highly excited silicon,” Appl. Phys. Lett., **31** (5), 346-348 (1977).
26. G. Augustine, A. Rohatgi, and N. M. Jokerst, “Base doping optimization for radiation-hard Si, GaAs, and InP solar cells,” IEEE Trans. Electron Dev., **39** (10), 2395-2400.

http://www.springer.com/978-1-4939-2750-0

Silicon Analog Components
Device Design, Process Integration, Characterization, and Reliability

El-Kareh, B.; Hutter, L.N.
2015, XLI, 607 p. 454 illus., Hardcover
ISBN: 978-1-4939-2750-0